Title
ANGULAR DISTRIBUTION OF NEUTRONS PRODUCED BY 40-AND 80-MeV a PARTICLES ON A THICK TANTALUM TARGET

Author
Wadman, William W.

Publication Date
1964-05-01

UCRL-11375 Rev.

University of California

Ernest O. Lawrence Radiation Laboratory

ANGULAR DISTRIBUTION OF NEUTRONS PRODUCED BY 40- and 80-MeV α PARTICLES ON A THICK TANTALUM TARGET

Berkeley, California

DISCLAIMER

To be published in Health Physics

UCRL-11375 Rev.

UNIVERSITY OF CALIFORNIA

Lawrence Radiation Laboratory
Berkeley, California

AEC Contract No. W-7405-eng-48

ANGULAR DISTRIBUTION OF NEUTRONS PRODUCED BY 40- and 80-MeV α PARTICLES ON A THICK TANTALUM TARGET

William W. Wadman

May 1964

ANGULAR DISTRIBUTION OF NEUTRONS PRODUCED BY 40- and 80-MeV α PARTICLES ON A THICK TANTALUM TARGET*

William W. Wadman

Lawrence Radiation Laboratory
University of California
Berkeley, California

May 1964

ABSTRACT

The angular distribution of neutrons has been measured for 40- and 80-MeV (41.2 ± 0.4 and 80 ± 1, respectively) α-particle beams on a thick elemental tantalum target. The measurement employed six different types of threshold reaction detectors with thresholds ranging from 1.2 to 12.4 MeV. The detectors were spaced about a ring 30 cm in diam centered about the target.

The target was contained within a Faraday cup in order to measure the total beam current. High voltage applied to a guard ring which preceded the cup was used to suppress secondary electron emission.

Before irradiation of the detectors, the beam was shaped and centered while being watched by closed-circuit television during the alignment.

The irradiated threshold detectors were analyzed with a 3-in. -diam × 3-in. -long NaI(Tl) crystal and a 400-channel pulse-height analyzer. The resulting data clearly indicate the existence of a prominent forward-directed neutron flux. The forward predominance is more pronounced in the higher-threshold-energy detectors. The ratio of the 70° to 0° flux decreases with the energy at which a detector's reaction cross section is in its maximum region. This type of comparison is influenced by the shapes of the cross

sections as a function of energy for each type of detector.

The total fast neutron yield was calculated approximately by using the $^{58}Ni(n,p)\ ^{58}Co$ reaction and that neutron flux which would be necessary to achieve the measured activity, and correcting for the anisotropy of the forward hemisphere. The neutron yield as a function of energy appears reasonable when compared with data of Allen et al.

I. INTRODUCTION

The angular distribution and yield of neutrons from 40- and 80-MeV α particles has been studied with several types of threshold detectors. The experiments were performed at the Berkeley heavy-ion linear accelerator and 88-inch cyclotron. Data were obtained for application to the design of a high-efficiency local neutron shield for each accelerator.

II. THE EXPERIMENT

The experiment involved a target of a selected material, a means of measuring the beam particle current, the selected threshold detectors, a device to mount the detectors at predetermined positions, and a means to suppress secondary emission electrons from escaping the current-measuring device. Incorporated as part of the accelerator beam pipe assembly, a quartz or phosphor screen was mounted to allow visual observation of the beam shape and centering during tune-up.

A. Threshold Detectors

The threshold detectors were selected on the basis of reaction threshold, reaction cross section, and half life. This is a part of a set of criteria established by Ringle[1] for the selection of 29 usable reactions involving 22 different isotopes from 17 different elements. Table 1 summarizes the threshold detectors and their various properties as used in this work.

Table 1. Threshold detector properties.

Reaction	Calculated threshold (MeV)	Peak cross section (barns)	Product half-life	Isotope (%)	Energy of a beam used (MeV)	Energy of γ-ray of reactant used for data (MeV)
$^{58}Ni(n,p)^{58}Co$	1.1	0.556	71 days	67.8	40, 80	0.81
$^{59}Co(n,\alpha)^{56}Mn$	5.4	0.112	2.6 hrs	100	80	0.845
$^{65}Cu(n,p)^{65}Ni$	4.1	0.035	2.6 hrs	30.9	80	1.5
$^{27}Al(n,\alpha)^{24}Na$	6.7	0.243	15 hrs	100	40, 80	1.37
$^{203}Tl(n,2n)^{202}Tl$	8.5	2.78	12 days	29.5	80	0.44
$^{127}I(n,2n)^{126}I$	9.5	2.02	13 days	100	40, 80	0.65
$^{58}Ni(n,2n)^{57}Ni$	12.4	0.25	37 hrs	67.8	80	1.36

For various technical reasons, it proved impossible to use all the detectors for the 40-MeV run.

B. Detector Mounting

The threshold detectors were mounted on a brass ring 30 cm in diameter. The ring was designed to be clamped directly to the beam pipe. The assembly was mounted with the target position at the center of the ring. With this arrangement the detector's angular location was known to ± 1%.

C. Target Material

The target material was selected on the basis of information by Tai et al.[2] for a target of relatively abundant neutron yield, and of Allen et al.[3] on broad angular total yield of neutrons.

The target was made of tantalum, and measured 2.5 in. in diameter and 0.25 in. thick. This dimension was adequate for stopping the α particles and for covering the end of the copper Faraday cup in which it was mounted.

D. Beam Current Measurements

The Faraday cup was constructed of oxygen-free copper tubing, 1/8-in. wall, 2.5-in i.d., and 4 in. long. The cup was fastened to the mounting flange with 3/4-in.-long standoff insulators. Preceding the cup by 3/8 in. and on three standoff insulators was a ring of the same diameter and 1.5 in. long. To this ring was applied -1600 V, in order to suppress secondary electron emission from the target and Faraday cup to avoid an incorrect beam-current measurement.[4] This reduced a scattering and absorption problem which would be present if we used a large magnet to perform the same suppression function. Accuracy of this method is better than ±3% absolute. The beam current and high voltage were led through ceramic feed-throughs in the mounting flange. These were connected to appropriate electrical connectors.

E. Beam Tuning

Prior to the irradiation of the threshold detectors, the α-particle beam was tuned for minimum diameter and maximum current. The shape of the beam was determined visually, by use of a phosphor-coated Lucite plug fitted over the end of the beam pipe for the 40-MeV work done at the heavy-ion linear accelerator, and a quartz plate with etched graduations at the 88-inch cyclotron for the 80-MeV work. Both were observed with remotely controlled closed-circuit television while the beams were being tuned for position and shape. After the shape was made small enough and the beam was centered, the visual apparatus was removed and the Faraday cup with the tantalum target was bombarded. The beam current was then maximized.

A quick secondary check of stray beam was made by removing the high voltage from the suppressor ring and observing the ring with the integrating beam-current electrometer. If no beam current could be observed the leads were returned to their normal configuration and the ring with the threshold detectors was mounted and accurately positioned about the target. Thereafter, the integrating electrometer was reset and the bombardment proceeded. The beam-current variation was constantly observed by the operators. Long-term variations were held within 8%, although short-term variations of less than 2 minutes were as much as 50%.

III. ANALYSIS OF THE DETECTORS

The irradiated threshold detectors were counted with a 3-in. -diam × 3-in. sodium iodide (NaI) crystal in a matched window configuration, coupled to a 400-channel pulse-height analyzer. This spectrometer was calibrated at least daily with a ^{137}Cs or ^{40}K source. The pulse-height analyzer was housed in a fully air-conditioned and humidity-controlled room.

The NaI crystal was mounted inside a cave made of solid blocks of serpentine. (Serpentine is a natural mineral material that has been found to contain very little if any radioactivity.[5]) The background counting rate inside the serpentine cave is 450 counts per minute for the 400-channel background spectrum, from 0.080 to 4.32 MeV.

Each threshold detector was counted at 3.0 cm from the actual face of the NaI crystal. The resultant γ-ray spectra were used during the reduction of the data.

IV. RESULTS

The reduction of γ-ray spectra to neutron density and energy interval was performed in essentially the following order.

The appropriate γ-ray energy photopeaks were selected in accordance with the product of the reaction in the threshold detector. The counts in appropriate channels of the spectrometer readout were summed so that the same energy interval was used for each γ ray of a given energy. From the summed photopeak were subtracted both the background and the Compton distribution from higher-energy γ rays in the spectrum.[1,6]

The total counts in the photopeak were corrected for decay and saturation. A correction was made for the abundance of the γ ray for the decay scheme for each type of disintegration.[7,8] The foils were weighed before irradiation to the nearest 0.1 mg, and the weight was corrected for percent of the threshold isotope present. This allowed the results to be put in terms of 1.02×10^{22} atoms of the threshold reaction isotope, when weight was applied as a factor to the isotope's density. This process normalized all data to 1 gram of nickel.

In both accelerator beam alignments, circumstances were such that we had to accept an offset beam. Fortunately this was only a horizontal displacement. This offset was corrected for by calculating the flux density for the different radii involved, using the inverse-square relationship. The actual angle at which the threshold detector lay with respect to the new beam center is incorporated in the data. The 40- and 80-MeV irradiation rates were normalized to 1-μA rates. The data were corrected for counting geometry and total absolute efficiency for the size of the NaI crystal, γ-ray energies, distance of the sample from the crystal, and sample size and thickness.[14]

A center-of-mass (c.m.) transformation was considered for purposes of comparison; however, we were interested mainly in the laboratory system. It is considered that such a transformation would not be as meaningful in light of the target thickness and preproduction α-particle scattering, incident energy degradation, and postproduction neutron scattering and energy degradation prior to detection in the threshold detectors. Lastly, the relative masses of the target and projectile nuclei cause a relatively small change in the transformation from the lab to the c.m. system. Hence, the data will be considered only in the laboratory system.

In order to attempt an intercomparison of the relative neutron flux necessary to produce the observed and corrected activities for each type of threshold detector, a broad assumption was made. On the basis of the calculated highest value of reaction cross section for the desired reaction,[1] a ratio to one barn was determined, and all data were corrected accordingly. The resultant information was arranged in the order of the energy at which the reaction cross-section peak occurred and was found to be generally acceptable.

A. Neutron Flux and Angular Distribution

The neutron flux for each threshold detector was calculated in the accepted manner on the basis of total absolute activity and cross section.

The plots of the angular distribution of neutrons are shown in Figs. 1 and 2 for the 40-MeV and 80-MeV α-particle bombardments, respectively. The plots are of the calculated neutron flux as a function of laboratory angle for the various threshold detectors used. In this manner of presentation, the integrated neutron flux greater than the reaction threshold energy can be more easily recognized. When one compares the data according to energy

for the highest value of reaction cross section, the copper data seem low and the iodine data seem high. For lack of more threshold detector information, the 40-MeV data appear reasonable. One might expect a larger difference between the data for aluminum and iodine in light of the observation of the 80-MeV information. The uncertainties in the values of the reaction cross section and the relation of each foil's neutron flux to that peak value may introduce uncertainties that range over a factor of five. (See Appendix and Figs. 10 and 12.) Conversion from photopeak counts to neutron flux is considered to be ± 15% with the exceptions of the copper, iodine, and thallium (n, 4n) data. The counting statistics for the photopeaks vary from 0.29 to 3.93%, except for ^{200}Tl, which vary from 2.4 to 37.9%. All variations affect the entire set of threshold detector data, and do not change the shape of the curve.

The relative distributions of neutrons as a function of angle are plotted in Figs. 3 and 4. The polar-coordinate relations of all the detectors are normalized to zero degrees. It becomes apparent that the peak reaction cross-section value is somewhat more influential on the shape of the distribution than the threshold energy. The relation between any point on the relative plots and the flux plots of Figs. 1 and 2 is easily determined either by direct comparison or from the multiple of the 0° flux and the relative value of Fig. 3 or 4.

Figure 5 is a plot of the ratio of the 70° to 0° flux. The results tend to indicate fairly good agreement between threshold detectors in terms of the energy for the highest value of reaction cross section. Strong evidence is indicated here for agreement with the methods of comparison and reduction. As shown in Fig. 5, all ratios of the foils fall on a semilogarithmic line except for the threshold detector which would be most strongly affected by

scattered neutrons, $^{58}Ni(n,p)\ ^{58}Co$ in the 80-MeV case. The 40-MeV scattering problem was considerably less.

An interesting point to note is the inclusion of the $^{203}Tl(n,4n)\ ^{200}Tl$ reaction values obtained from the 80-MeV bombardment. The calculated threshold for this reaction is about 27.5 MeV. (The cross section as a function of energy cannot be calculated with the computer program now in use here. [4])

B. Fast Neutron Production

Using the low-energy nickel reaction data for the total integrated flux, one can calculate the approximate fast-neutron yield that resulted from each bombardment. Knowing the irradiation distance of 15 cm, and the calculated neutron flux as a function of angle, one can treat the data in terms of the inverse-square relationship, and the emission (Ω) can be evaluated.

For ease in calculating Ω, the change of the slope of neutron flux as a function of angle was considered to be a simple exponential, although the data did display a slight variation. Accounting for the variation would not change the resultant Ω by more then 5%. The evaluation follows:

$$\Omega = \int_0^{\pi} \phi(\theta)\, 2\pi r^2 \sin\theta d\theta$$

$$= 2\pi r^2 \int_0^{\pi} \phi(\theta) \sin\theta d\theta$$

$$= 2\pi r^2 \phi_0 \int_0^{\theta_1} e^{-a\theta} \sin\theta d\theta + 2\pi r^2 \phi_k \int_{\theta_1}^{\pi} \sin\theta d\theta$$

$$= 2\pi r^2 \phi_0 \left[\frac{e^{-a\theta}(-a \sin\theta - \cos\theta)}{a^2+1} \right]_0^{\theta_1} - 2\pi r^2 \phi_k \cos\theta \Big|_{\theta_1}^{\pi}, \quad (1)$$

where

r = 15 cm,

ϕ = n/cm^2-sec · μA,

θ = angle from incident beam (radians),

a = 0.9856 for 80-MeV α on Ta

= 1.022 for 40-MeV α on Ta,

ϕ_k = flux constant, minimum value of ϕ,

and θ_1 = angle beyond which ϕ_k exists (≈ 60°).

The total emission in terms of 4π steradians for the work with 40-MeV alpha on tantalum was evaluated at $Q = 1.96 \times 10^{10}$ n/sec-μA. The yield for 80-MeV α beam on tantalum was evaluated as $Q = 3.0 \times 10^{11}$ n/sec-μA. Both values are approximate, as the method of determination was the use of the ^{58}Ni(n, p) reaction. The threshold, 0.01 of the peak reaction cross-section energy, is 1.1 MeV. The results should be accurate to ±25%.

In comparing the two parts of the integration in equation (1), it was noted that for both α-particle energies, approximately 55% of the total emission passed through the forward two steradians. The ratio of the Q's (emission) is 16:1. This is considerably higher than the 8:1 ratio that the author has measured with a long counter for 50- and 100-MeV alphas. In the attempt to explain the difference in production ratios between these data and the long-counter data, several good explanations were brought forth. The most satisfactory seemed to be that offered by Harvey,[10] which deals with the reaction Q for (α, xn) in tantalum. Apparently the (α, 1n) reaction has a very small probability because the required energy is smaller than the Coulomb barrier

of the system. Neutron production becomes evident with alphas greater than about 20 MeV. The production threshold is also about the energy region of (α,2n) for tantalum, and so the x increases, as it is controlled by the energy available in the compound-nucleus system.[11]

In comparing the foregoing with these data, one data point for neutron yield for thick targets was found in Allen et al.,[3] and although it is an extrapolation, it tends to confirm the explanation by Harvey.[10] Figure 6 shows the three total-neutron-yield points as a function of α-particle energy. Also plotted is an 8 to 1 production-increase line through the 50- and 100-MeV α points in the curve.

APPLICATION OF RESULTS

Application of the results of this information is in the design of a local shielding configuration for the two accelerators mentioned. The work presented here was studied simultaneously with attenuation characteristics for the same neutron energies, and the resultant effectiveness of various thicknesses of shielding was determined for 0° and 90°.

One of the criteria for local shielding of the sources of neutrons in an experimental cave is that one man, of average strength, be able to move it. This required that the large attenuators be constructed of several independently movable pieces.

The reduction of neutron flux with increasing angle and the strong forward predominance of the high-energy neutron component prompted a tentative design of the shield configuration that is about 3 feet thick in the forward direction and 1 foot at 90°. The mass was considered to be divided into three parts: a cylinder to fit over the Faraday cup, and two discs of 18 in. of concrete to fit against the end of the cylindrical shield. Each would

be on its own tapered frame which is broader at the bottom to lower the center of gravity, and narrower at the front to allow one set of wheels and the frame to roll partly into the other frames. The shield for midstream collimators and for targets enclosed in small apparatus consists of two half cylinders which are brought together from the opposite sides of the beam pipe or structure. These shields also will rest on tapered frames such as those mentioned previously. Obviously the taper must be oriented to permit the two to fit together.

Results of actual tests of these shield configurations will be obtained during the fall and winter of 1964, and information will be published shortly thereafter.

ACKNOWLEDGMENTS

The author wishes to thank the members of the Health Physics Department for information and ideas that contributed to this project. In particular, I would like to thank Captain Walter Gundaker and David Pietenma for their aid during all phases of the 40-MeV work; Alan R. Smith for helpful suggestions dealing with γ spectroscopy, and him and John Ringle for threshold-detector information; Art Kohler for mathematical treatment of one part of the data; and Dr. George Igo, Dr. Bernard Harvey, and Dr. John Meriwether, for their stimulating discussions and continued encouragement throughout various phases of this project.

REFERENCES

* Work done under the auspices of the U.S. Atomic Energy Commission.

1. John Clayton Ringle, Techniques for Measuring High-Energy Neutron Spectra Using Threshold Detectors (Ph.D. Thesis), Lawrence Radiation Laboratory Report UCRL-10732, October 11, 1963.
2. Yuin-Kwei Tai, George P. Millburn, Selig N. Kaplan, and Burton J. Moyer, Neutron Yields from Thick Targets Bombarded by 18- and 32-MeV Protons, Phys. Rev. 109, 6 (1958).
3. A. J. Allen, J. F. Nechaj, K. H. Sun, and B. Jennings, Thick Target Fast Neutron Yield from 15-MeV Deuteron and 30-MeV Alpha Bombardment, Phys. Rev. 81, 4 (1951).
4. John R. Meriwether (Lawrence Radiation Laboratory), private communication.
5. Harold A. Wollenberg and Alan R. Smith, Earth Materials for Low-Background Radiation Shielding, Lawrence Radiation Laboratory Report UCRL-9970, May 24, 1962.
6. R. L. Heath, Scintillation Spectrometry Gamma-Ray Spectrum Catalogue, Phillips Petroleum Company Report IDO-16408 (TID-4500), July 1, 1957.
7. D. Stominger and J. M. Hollander, Decay Schemes, Lawrence Radiation Laboratory Report UCRL-8289, June, 1958.
8. D. Stominger, J. M. Hollander, and G. F. Seaborg, Table of Isotopes, Rev. Mod. Phys. 30, #2, Pt. 2, (1958).
9. D. J. Hughes and R. B. Schwartz, Neutron Cross Sections, Brookhaven National Laboratory Report BNL-325, January, 1957.

10. Bernard G. Harvey (Lawrence Radiation Laboratory), private communication.

11. J. D. Jackson, Can. J. Phys. 34, 767 (1956).

12. J. M. Blatt and V. F. Weisskopf, Theoretical Nuclear Physics, Chapter VIII. Wiley, New York, (1952).

13. R. G. Moore, Jr., Nuclear Reaction Cross-Section Theory, Rev. Mod. Phys. 32, 101 (1960).

14. S. H. Vegors, Jr., Louis L. Marsden, and R. L. Heath, Calculated Efficiencies of Cylindrical Radiation Detectors, IDO-16370, September, 1958.

FIGURE CAPTIONS

Fig. 1. Angular distribution of neutrons from the 40-MeV α-particle bombardment of a thick tantalum target. Neutron flux at 15 cm as a function of laboratory angle for nickel, aluminum, and iodine threshold detectors.

Fig. 2. Angular distribution of neutrons from the 80-MeV α-particle bombardment of a thick tantalum target. Neutron flux at 15 cm as a function of laboratory angle for nickel (n, p), copper, aluminum, cobalt (n, α), thallium (n, 2n), iodine, nickel (n, 2n), and thallium (n, 4n), reactions.

Fig. 3. Angular distribution of neutrons from the 40-MeV α-particle bombardment of a thick tantalum target. All detectors are normalized to 0°.

Fig. 4. Angular distribution on neutrons from the 80-MeV α-particle bombardment of a thick tantalum target. All detectors are normalized at 0°.

Fig. 5. Ratio of 70° neutron flux to 0° neutron flux for both the 40-MeV and 80-MeV α-particle bombardments of tantalum.

Fig. 6. Total neutron production for 30-MeV, 40-MeV, and 80-MeV α particles on tantalum (30-MeV α data from Allen et al.) and the 8:1 ratio line plotted through the 50- and 100-MeV energy points, as measured with a long counter.

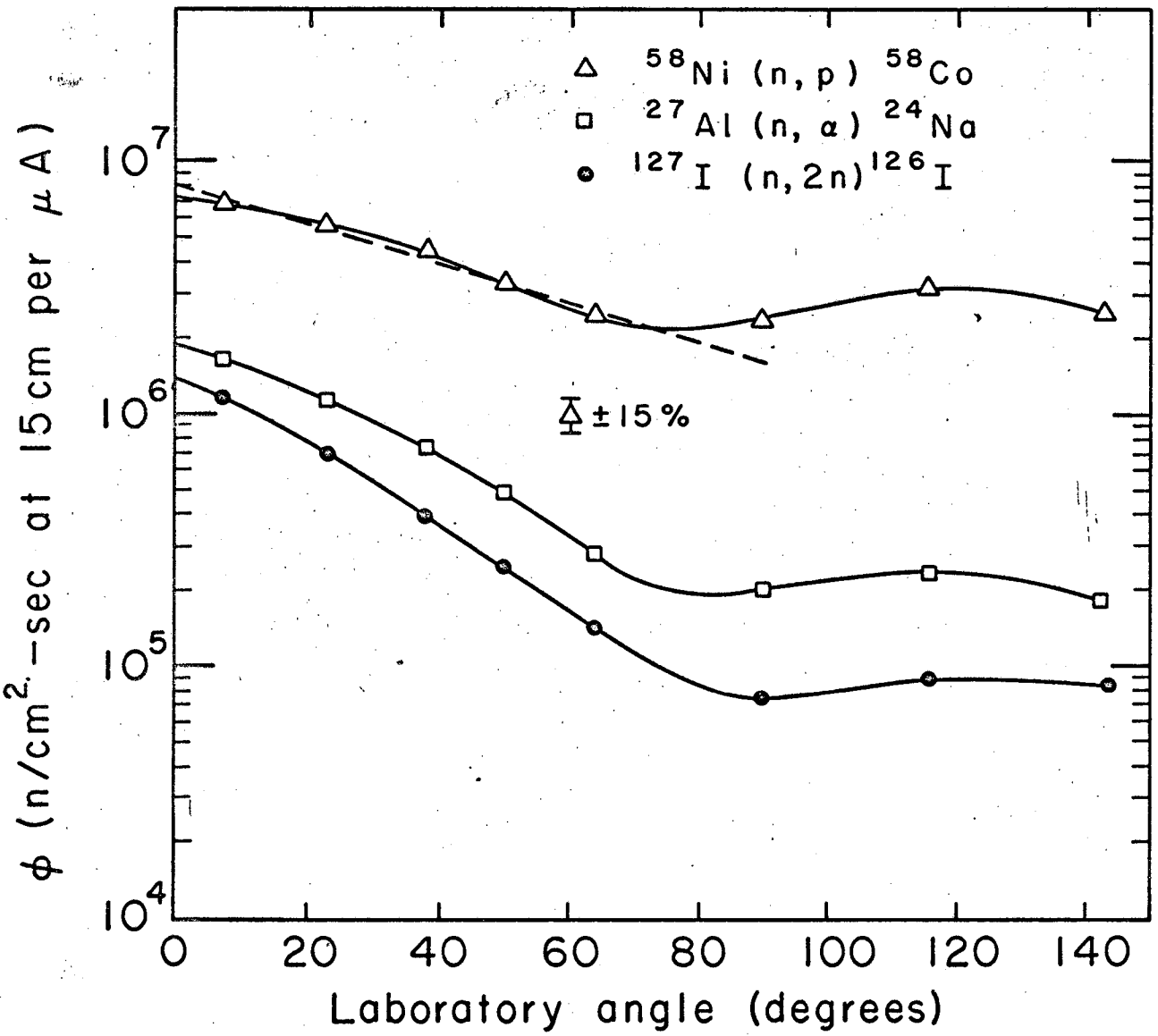

Fig. 1

MUB–2891

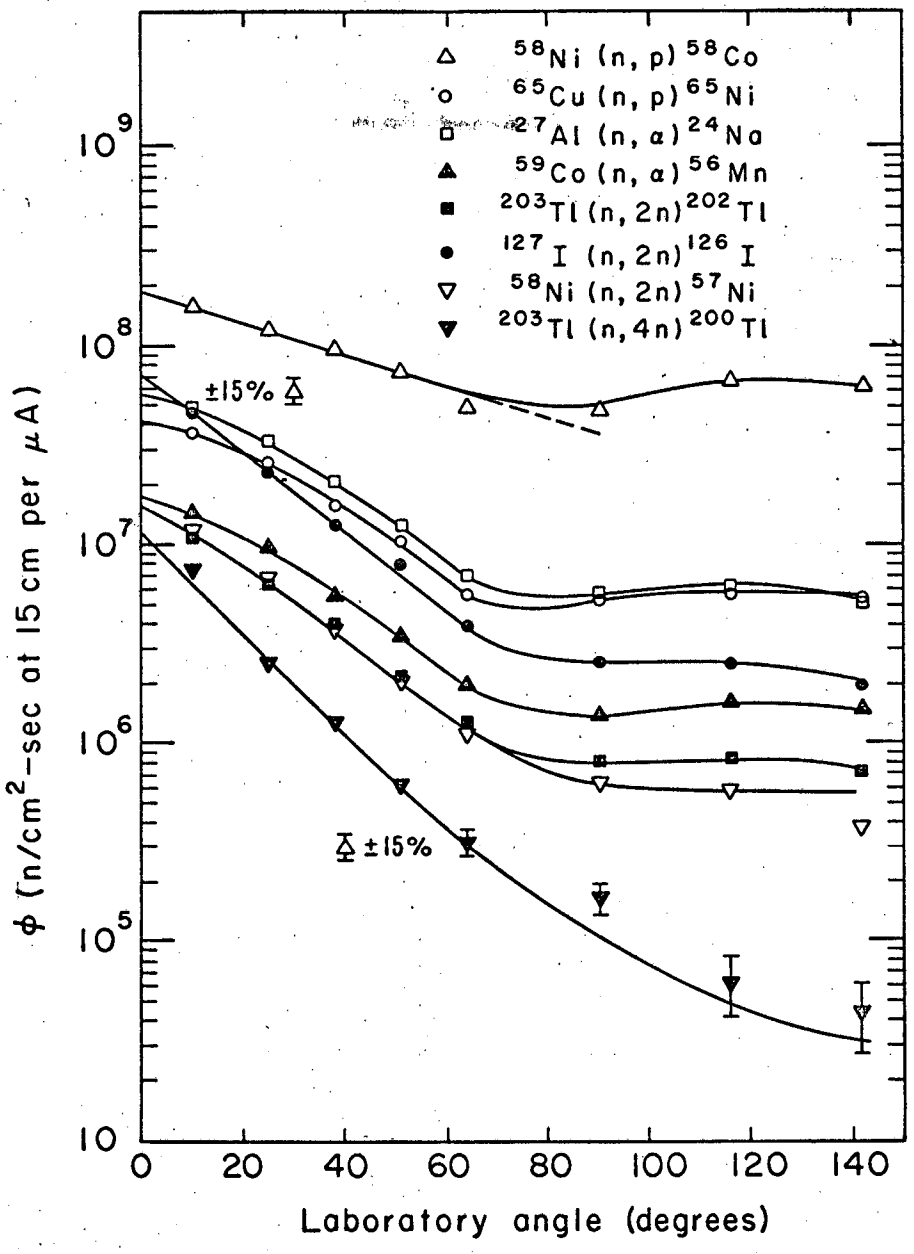

Fig. 2

MUB-2892

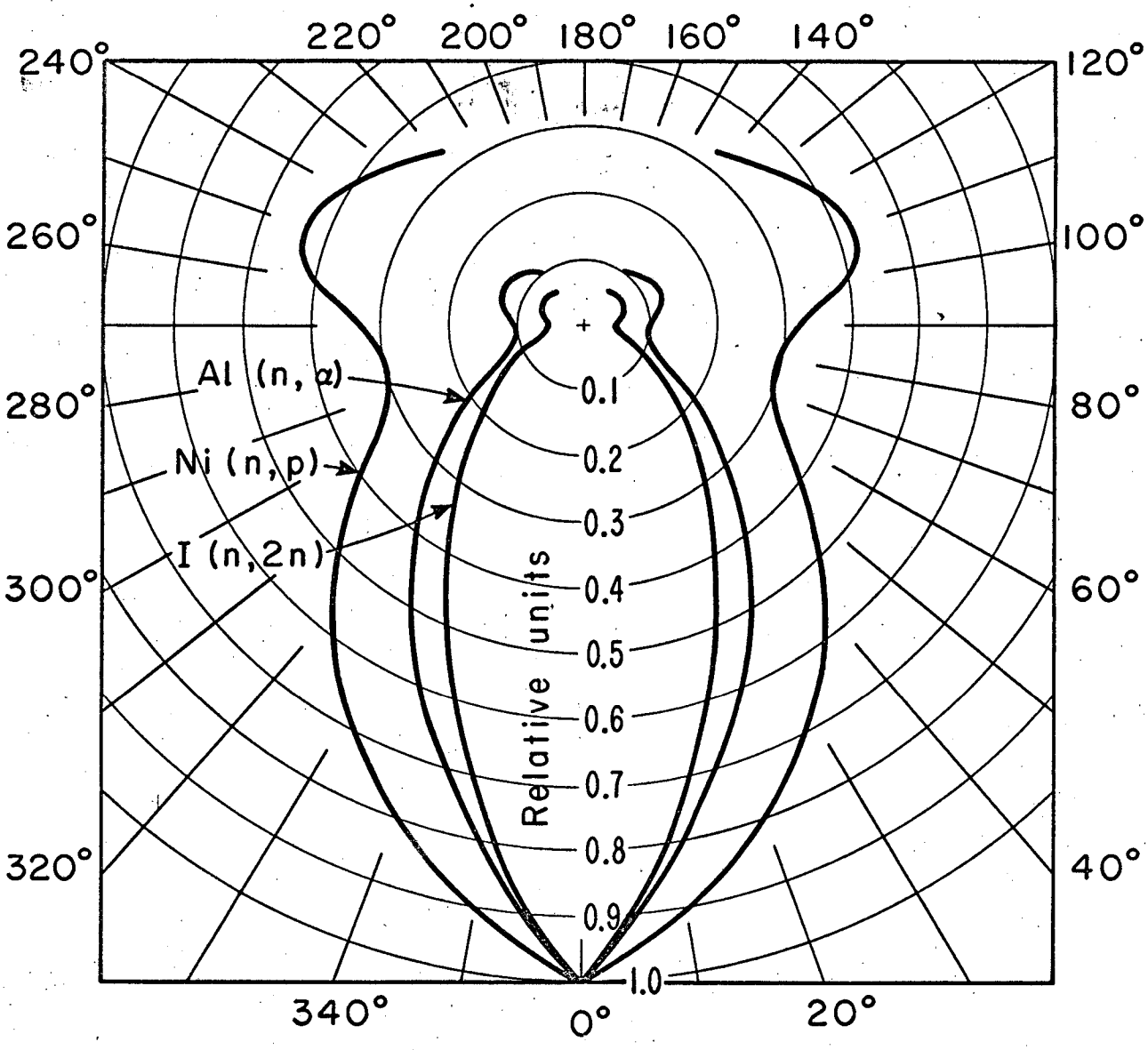

Fig. 3

MUB-2893

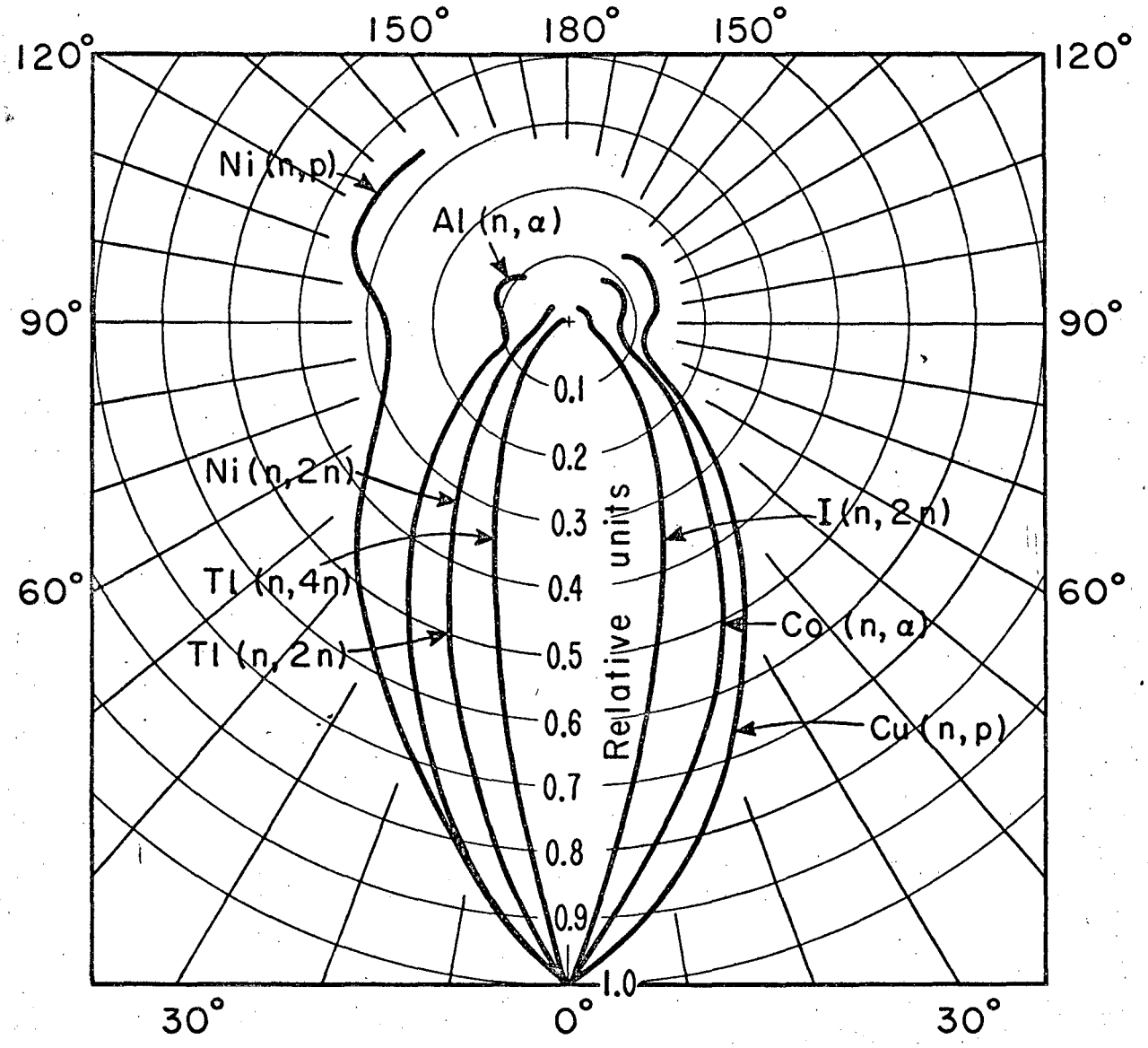

Fig. 4

MUB-2894

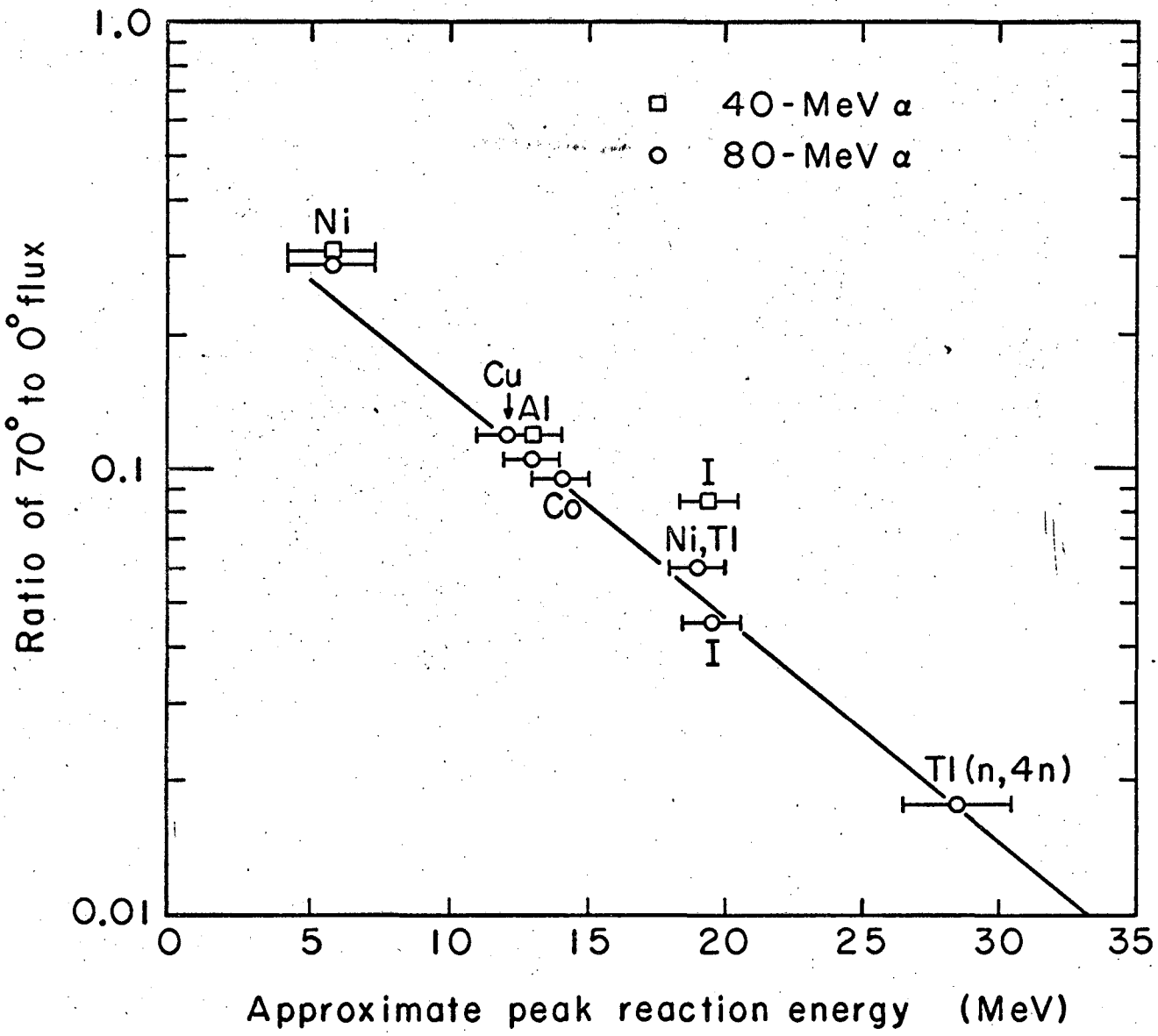

Fig. 5

MUB-2895

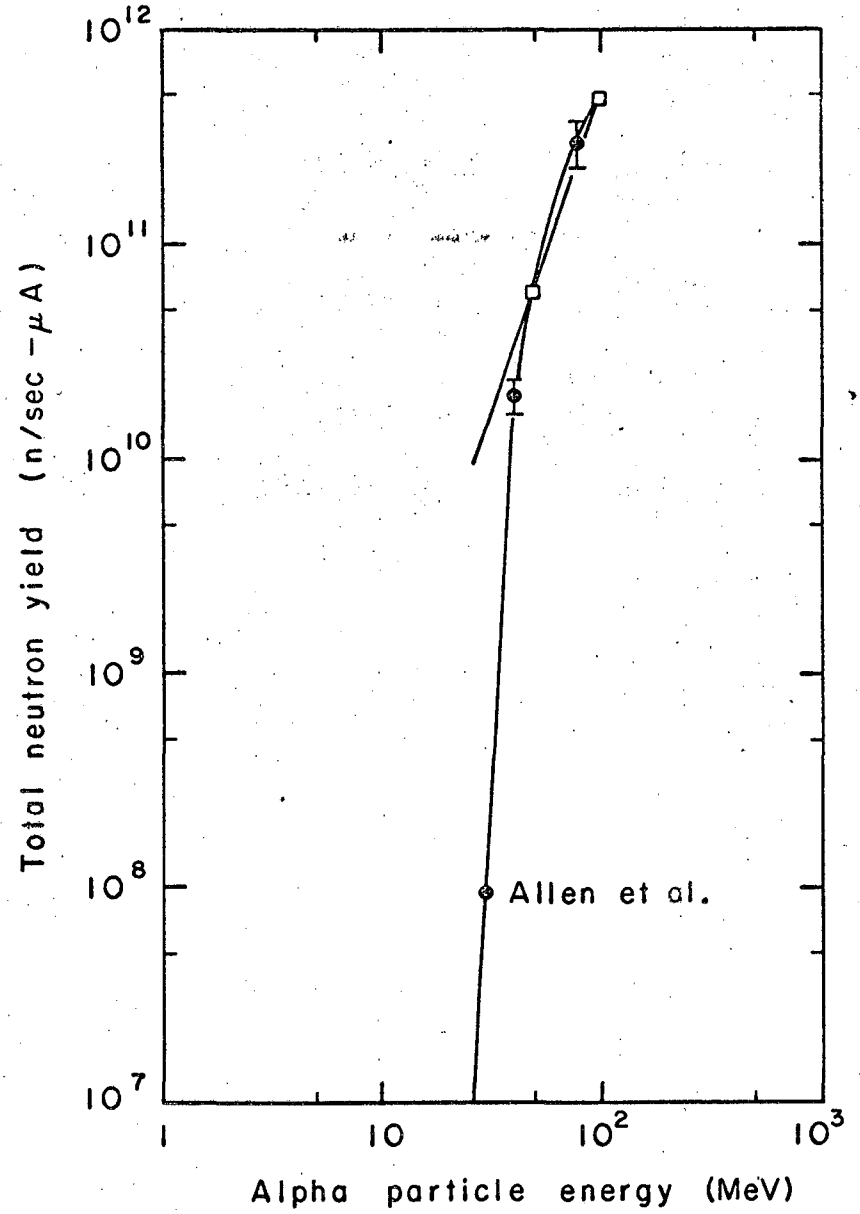

Fig. 6

MUB-2896